International Journal of Material Forming (2025) 18:3
https://doi.org/10.1007/s12289-024-01867-3

ORIGINAL RESEARCH

The influence of the adiabatic heating coefficient on the near solidus forming process

Muhammad Sajjad[1] · Julen Agirre[1] · Gorka Plata[1] · Jokin Lozares[2] · Joseba Mendiguren[1]

Received: 15 July 2024 / Accepted: 19 November 2024

Abstract

The Near Solidus Forming (NSF) process represents a critical method for shaping metallic components under extreme temperature conditions. When metals deform plastically, significant amounts of heat can be generated, which is due to the conversion of plastic deformation energy in the material often known is adiabatic heating. In this study, the influence of the adiabatic heating coefficient (AHC) on temperature distribution and plastic strain during NSF process is investigated. For this purpose, three industrial benchmarks previously fabricated using NSF techniques are selected to serve as representative cases for analysis. To conduct the analysis, sensitivity studies is performed at two key temperatures: 1360 °C and 1370 °C. These temperatures are chosen to capture the range of operating conditions typically encountered in industrial NSF applications. The simulation tool FORGE NXT® is utilized to investigate the potential effect of AHC on equivalent plastic strain (EPS). The range of potential AHC values considered is between 85% and 100%, as determined from a comprehensive literature survey. The study suggests that the AHC has a minimal effect on the deformation behaviour of 42CrMo4 steel at NSF condition for the studied benchmarks. The findings of this study provide the inside to the importance of AHC in the developing of a reliable Digital Twin (DT) for industrial NSF application.

Keywords Near solidus forming (NSF) · Adiabatic heating coefficient (AHC) · FORGE NxT® · Equivalent plastic strain (EPS) · Digital Twin (DT)

Introduction

The Near Solidus Forming (NSF) process is performed at temperatures close to the solidus temperature of the material. This process offers advantages such as low forming forces and reduced material waste since it is conducted at high temperatures in a single stage compared to traditional hot forming [1]. Given the significant benefits of NSF over traditional forming techniques, understanding material behaviour under extreme conditions of temperature and pressure is essential. Among the various factors influencing material response during the forming process, adiabatic heating is critical [2]. Adiabatic heating in the forming process arises from the conversion of deformation energy into heat within the workpiece material during plastic deformation [3]. This heating impacts the temperature profile during the forming process, which can significantly affect processes that are highly sensitive to temperature [4].

In theory when the temperature rises within the workpiece, flow properties such as flow stress and strain rate sensitivity adjust accordingly, which is generally observed

✉ Muhammad Sajjad
msajjad@mondragon.edu

Julen Agirre
jagirreb@mondragon.edu

Gorka Plata
gplata@mondragon.edu

Jokin Lozares
jokin.lozares@deusto.es

Joseba Mendiguren
jmendiguren@mondragon.edu

[1] Faculty of Engineering, Mechanics and Industrial Production, Mondragon Unibertsitatea, Loramendi 4, Mondragon, Gipuzkoa 20500, Spain

[2] Department of Mechanics, Design and Industrial Management, University of Deusto, Avda. of Universities 24, Bilbao 48007, Spain

Published online: 04 December 2024

across various alloys, as discussed in studies on high-entropy alloys and medium manganese steel [5, 6]. For example, in 42CrMo4 steel [7], as with other metals at elevated temperatures from adiabatic heating can induce thermal softening or even dynamic recrystallization, leading to changes in microstructure and mechanical properties, as seen in similar studies involving thermomechanical behavior in alloys like Ti6Al4V [8]. These microstructural changes can alter final product quality, including dimensional accuracy, surface finish, and mechanical integrity, which are essential considerations in 42CrMo4 steel applications. Moreover, the increased temperatures resulting from adiabatic heating can accelerate tool wear and degradation in hot forming, posing challenges for tool life and maintenance, as Härtel et al. noted in their analysis of high-temperature forming [9].

In the NSF process, materials are shaped at temperatures just below their solidus point, where they remain solid but are highly susceptible to deformation. The NSF process involves careful control of temperature to avoid phase transformations that can significantly affect the microstructure and mechanical properties of the final product. One of the principal guidelines in NSF is maintaining the temperature at a controlled level to minimize undesirable phase changes and optimize formability and final product characteristics [10]. Adiabatic heating where the increase in temperature due to plastic work during forming plays a crucial role in this process. Depending on the extent of heating, adiabatic effects can either stabilize or destabilize microstructure development, which directly impacts both the control of the forming process and the quality of the end product [11].

In high-temperature NSF operations, especially near the material's solidus temperature, adiabatic heating can have pronounced effects. Even minor variations can influence temperature distribution, flow behavior, and microstructural evolution, making precise temperature management essential to prevent localized overheating and ensure uniform properties in the final component [12, 13]. Thus, controlling adiabatic heating in NSF processes is critical to achieving consistent product quality and optimizing process efficiency.

Hodowany et al. (2000) conducted a comprehensive study on this topic, emphasizing the role of the adiabatic heating coefficient (AHC) as a key material parameter that governs the conversion rate of deformation energy into heat [14]. The AHC value, which varies by material and processing conditions, indicates the proportion of mechanical energy transformed into thermal energy during deformation. An AHC of 100% signifies full conversion, meaning all the deformation energy increases the material's internal temperature, while an AHC of 50% indicates that only half the deformation energy is converted to internal heating. Understanding and controlling AHC in high temperature forming process is essential for instance, high AHC values can lead to rapid temperature increases, potentially causing unwanted microstructural transformations or weakening in the material, while lower AHC values may demand additional energy input to reach optimal forming temperatures.

Different ranges of the coefficient have been considered by various authors. For instance, Mason et al. examined the range between 40% and 90% across materials such as steel, aluminium, and Ti-6Al-4 V titanium alloys subjected to high strain deformation [15]. Similarly, Kapoor et al. characterised the AHC equivalent to 85% during high-speed compression tests with estimated strain rates of approximately 3000 s^{-1} [16]. Hodowany et al. utilized a range between 75% and 100% in their investigation of Ti alloys during compression tests [17]. In summary, the literature presents diverse ranges of the AHC, which were selected based on factors such as the deformation rate and other boundary conditions.

Furthermore, various authors have used multiple techniques to characterise the AHC. For instance, Gao et al. utilized Differential Scanning Calorimetry (DSC) to measure heat flow into or out of a sample as a function of temperature or time during plastic deformation [18]. In DSC analysis, the heat capacity and thermal conductivity of the material are characterised, which are crucial parameters for calculating the AHC. Similarly, high-speed cameras with advanced image analysis techniques have been implemented for real-time observation of temperature changes and deformation during the forming process [19]. Due to the high complexity of these methodologies, some authors have opted for analytical modelling to characterise the AHC. For example, Paul et al. used the approach for the uniaxial tension of a slender metal rod, where material properties, deformation conditions, and heat transfer mechanisms are considered to derive equations describing the relationship between mechanical energy input and temperature rise, thereby estimating the AHC [20]. As expected, the analytical approach offers a faster initial assessment but with limited accuracy.

On the other hand, finite element analysis (FEA) is a prominent numerical tool for simulating hot forging processes, providing insights into temperature distribution, stress-strain behaviour, and energy dissipation within both the workpiece and dies [21]. Advanced constitutive models, including those integrating thermal softening and strain rate sensitivity, enable precise predictions of material behaviour under high-speed deformation, as demonstrated by Chadha et al. during ingot breakdown operations at high temperatures [22]. Similar approaches can be found throughout the literature for the characterization of high temperature forming processes. For instance, Sajjad et al. developed a digital twin for the NSF process, highlighting the utility of numerical methods in this domain [23]. These numerical methods allow for predicting the behaviour of the forming process

under different scenarios, such as varying temperatures, pressures, and other boundary conditions, without the need for costly and time-consuming physical experiments.

It is clear from the literature that the effect of adiabatic heating in various forming processes is investigated in term of AHC. Moreover, the effect of the AHC could be significant especially at high temperature conditions like NSF, therefore characterization of its impact for the development of reliable DT could be critical. Furthermore, the characterization techniques such as DCS analysis, high speed camera and analytical modelling is costly and time consuming. Therefore, prior to conducting experiments to investigate the impact of AHC, it is essential to develop a strategy capable of representing the importance of the AHC on the deformation behaviour in the NSF process while employing the characterised AHC ranges from the literature. In this way, the impact of the AHC on the NSF process is evaluated prior to the conducting costly and time-consuming experiments.

Given the gap in the literature, the main objective of this work is to evaluate the impact of the AHC in the NSF industrial process. To achieve this, three industrial benchmarks previously fabricated using the NSF process have been utilized. Sensitivity analysis is conducted at temperatures of 1360 °C and 1370 °C, employing 42CrMo4 steel material. The simulation tool FORGE NXT® is used to investigate the effect of potential AHC values on equivalent plastic strain and temperatures. The potential AHC used is ranged between 85% and 100% based on the literature study. To ensure a wide range of data, two boundary conditions for each benchmark, Low-bounds and High-bounds, were considered. The findings of this study will highlight the importance of AHC for the future development of an accurate DT for NSF industrial applications, which will serve as the cornerstone for the development and optimization of the material models for the NSF process in the industries.

Research methodology

The complete details of the research methodology are presented in Fig. 1. In this study, three industrial benchmarks (previously studied by the authors [23]) are consider. As from the work it can be stated, different boundary conditions can be assumed for these benchmarks, e.g. billet geometry, heat transfer coefficients, material behavior and etc.

In order to cover deformation at various boundary conditions two case-scenarios were defined depending on the boundary conditions: 'Low-bounds' and 'High-bounds'. Both case-scenarios were derived from the design of experiments (DOE) study outlined in the work of Sajjad et al. [23]. From this study, two extreme cases for each benchmarks experimental data were selected: one representing lower values (Low-bounds) and the other representing higher values (High-bounds). The Low-bounds represent the boundary conditions of the test where the plastic strain and forces are recorded lower during the test whereas higher in the case of High-bounds. A complete detail of the parameters and its levels for all benchmark cases are shown in Table 1. The reason for selecting the Low-bounds and High-bounds is to investigate the effect of adiabatic heating over a wide range of temperatures and plastic strain conditions. Furthermore, the adiabatic heating coefficient in the study is considered 85% ad 100% bsed on the literature survey for steel materials. Within this range the processes will be evaluated assuming AHC of 85% and also AHC of 100% with Finite Element Analysis (FEA). Lastly, the results from both boundary values of AHC are compared against each other to investigate its impact in the NSF process.

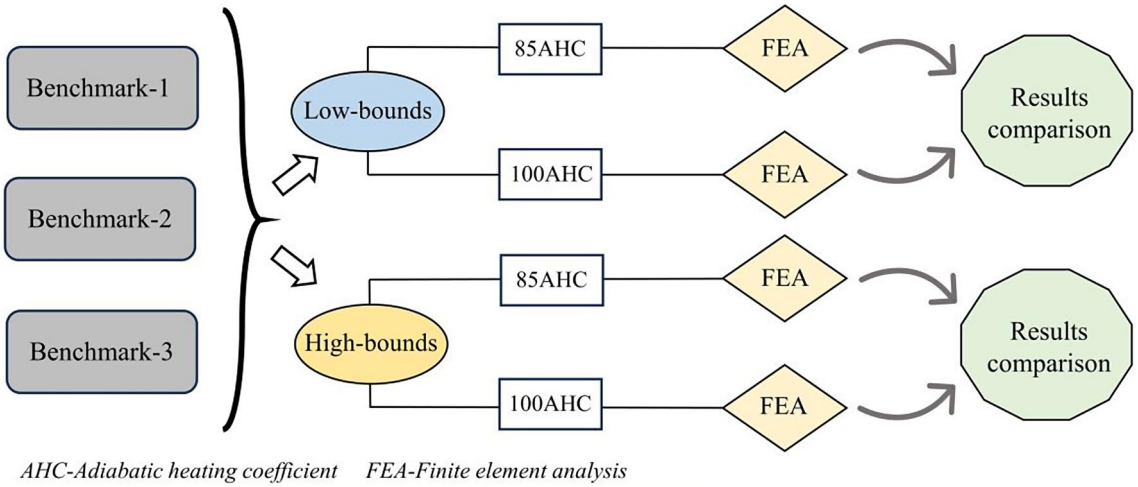

Fig. 1 Methodology schematic representation of the AHC analysis

Table 1 Configuration of input parameters and AHC of the Hook, H and R- spindle

Boundary condition	Low-bounds			High-bounds		
Industrial Component	HS	RS	HO	HS	RS	HO
Billet Diameter (mm)	64.7	68.8	64.7	65.3	69.3	64.7
Billet Length (mm)	89.5	92.5	92.5	90.5	92.5	93.5
Material	50%	50%	50%	100%	100%	100%
Billet Temperature (°C)	1360	1360	1360	1370	1370	1370
Dies Temperature (°C)	200	200	200	270	270	270
Heat Transfer Coefficient	2000	2000	2000	20,000	20,000	20,000
Emissivity	0.35	0.35	0.35	1.00	1.00	1.00
Ambient Temperature (°C)	50	50	50	70	70	70
Friction Coefficient	0.25	0.25	0.25	0.45	0.45	0.45

HS; H-spindle, RS; R-spindle, HO; Hook

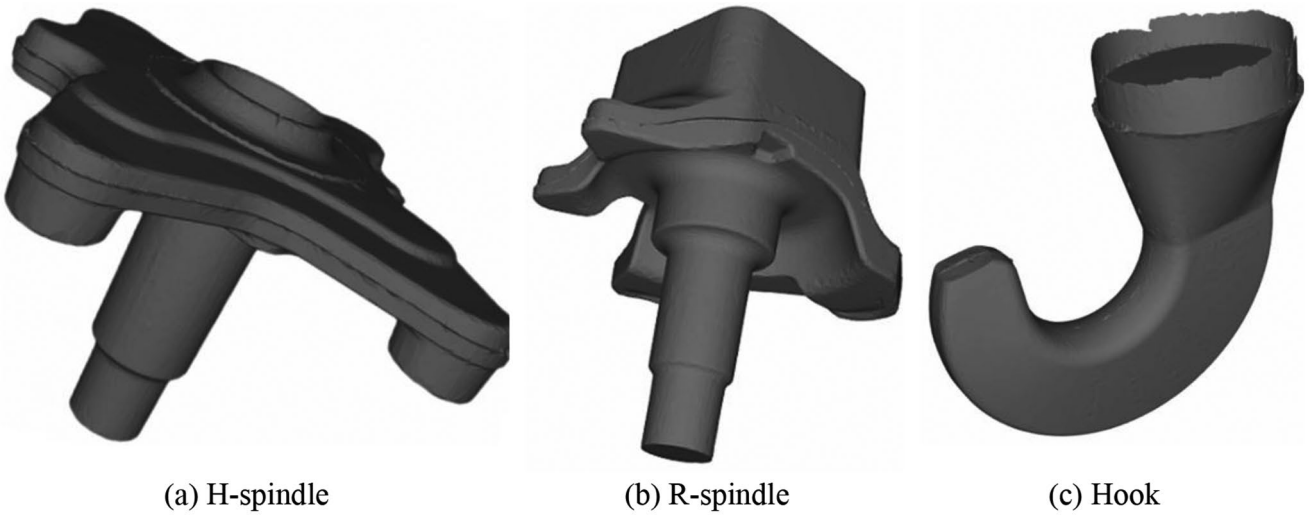

Fig. 2 NSF Industrial benchmarks

Industrial benchmarks

In this paper three industrial components such as R-spindle, H-spindle and Hook components were investigated, as shown in Fig. 2 [24]. The estimated weight of the components is ~2.3 Kg, ~3 kg, and ~2.4 kg respectively. All these components are fabricated from 42CrMo4 steel. More details about the components can be found in the work of Jokin et al., where he investigated the capability of the NSF process for the fabrication of automobile industrial components [10].

Numerical modelling of AHC study

For the simulation study, FORGE NxT® finite element software is used to develop the numerical models of all benchmarks as shown in Fig. 3(a). In the finite element analysis (FEM), Hansel–Spittel Constitutive model was introduced in Forge NxT® software and simulation at different boundary conditions were conducted. The Hansel–Spittel model describes the relationship between flow stress, strain, strain rate, and deformation temperature which was ideal for our case scenario and expressed by:

$$\sigma = Ae^{m_1 T}\varepsilon^{m_2}\dot{\varepsilon}^{m_3}e^{\frac{m_4}{\varepsilon}}(1+\varepsilon)^{m_5 T}e^{m_7\varepsilon}\dot{\varepsilon}^{Tm_8}T^{m_9}, \quad (1)$$

Where σ represents stress, ε denotes strain, $\dot{\varepsilon}$ is the strain rate, T is the deformation temperature, and m_1 to m_9 are material coefficients. In the context of NSF process the thermal aspects go beyond just the material's flow stress behavior such as the heat transfer between the workpiece and dies, and the surrounding air which plays a critical role in accurately simulating the temperature profile and its impact on deformation. The heat transfer between the hot workpiece and the cooler dies is primarily governed by conduction at the interface known as heat flux q across the die-workpiece interface and can be represented as:

$$q = h_c(T_{workpiece} - T_{dies}) \quad (2)$$

Where, h_c is the contact heat transfer coefficient between the die and the workpiece, $T_{workpiece}$ is the temperature of

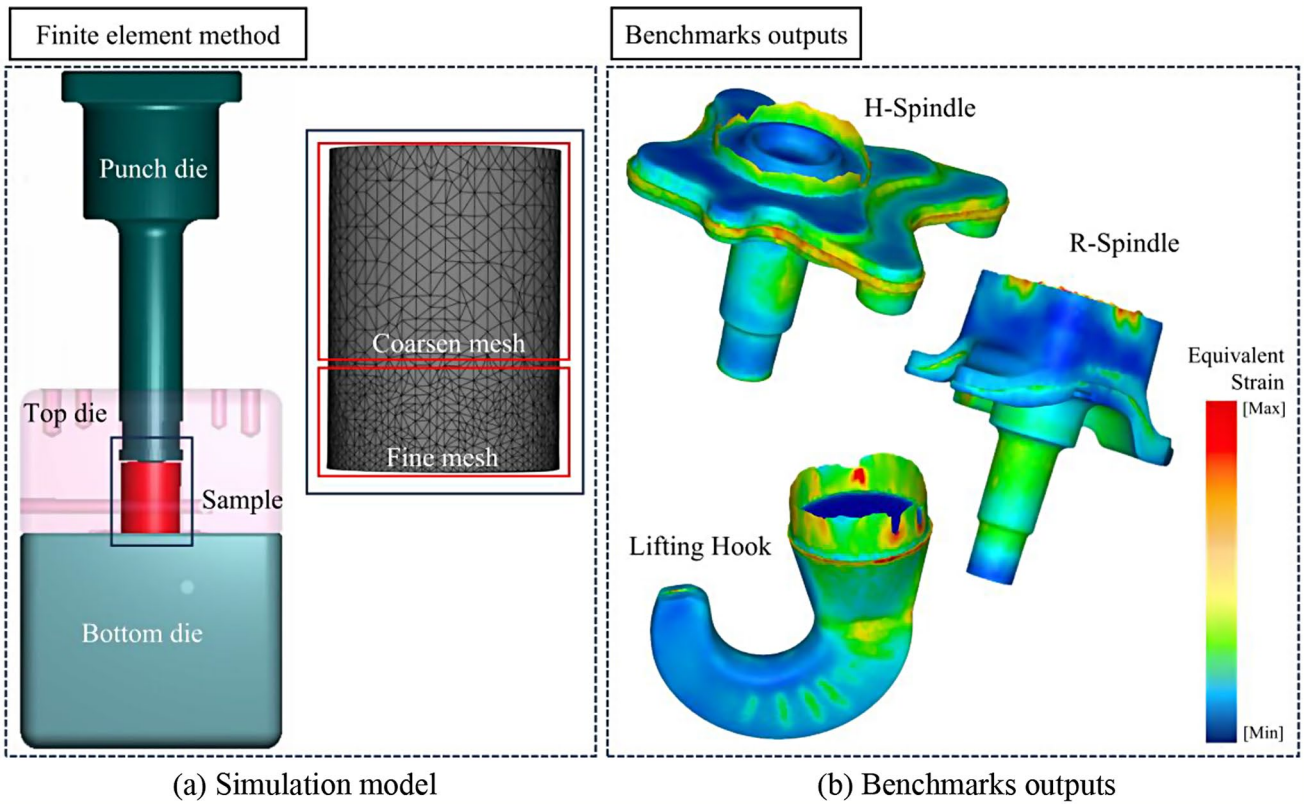

Fig. 3 Numerical analysis of the AHC study: (**a**) Simulation model (**b**) Benchmarks results (Equivalent Strain)

the workpiece surface and T_{dies} is the temperature of the die surface. The value of h_c vary significantly depending on factors like contact pressure, surface roughness, and lubricant conditions. However, in our case prior research on the NSF process, a heat transfer rate of 2000/or 20,000 W/m²K was established. To incorporate the heat transfer with the air the following equation were used which is expressed as:

$$\mathrm{q} = h_{air}(T_{workpiece} - T_{air}) \tag{3}$$

In this equation, h_{air} is the convective heat transfer coefficient to the surrounding air and T_{air} is the ambient air temperature. In high temperature forming process, h_{air} is always lower than h_c, as air is a poorer conductor compared to direct metal contact. Therefore, in the case of NSF the value is considered based on the study conducted prior for the characterization of the heat transfer at NSF testing conditions [25]. Furthermore, as the material undergoes plastic deformation, part of the work done on the material is converted into heat, raising its internal temperature. The rate of heat generation per unit volume noted as $\dot{Q}$ can be expressed as:

$$\dot{Q} = \beta.\sigma.\dot{\varepsilon} \tag{4}$$

Where, β is the Taylor-Quinney coefficient (typically around 0.85-1), representing the fraction of plastic work converted to heat, σ is the flow stress, $\dot{\epsilon}$ is the strain rate. Finally, the heat balance in the workpiece during deformation is represented by the heat conduction equation (assuming isotropic material properties):

$$\rho c_P \frac{\partial T}{\partial t} = k\nabla^2 T + \dot{Q} \tag{5}$$

Where, ρ is the material density, c_p is the specific heat capacity, k is the thermal conductivity of the material, $\nabla^2 T$ is the Laplacian of the temperature field, $\dot{Q}$ is the internal heat generation term due to plastic deformation (from the adiabatic heating equation). Overall, the equation represents the temperature distribution in the workpiece during deformation by considering heat conduction within the material, the adiabatic heat generation, and the heat loss at the boundaries due to conduction (with dies) and convection (with air). In conclusion while using the FORGE NxT®, the software often automatically incorporates these thermal relationships. However, the contact heat transfer coefficient h_c, the convective coefficient h_{air}, and setting accurate material properties (e.g., thermal conductivity, specific heat) as

per real-world conditions were specified to ensure a realistic simulation result.

The Fig. 3(b) represents the post deformed specimen of all benchmarks in the NSF process. In the simulation, the upper and lower tools were treated as rigid bodies, with unilateral contact and a prescribed heat transfer coefficient at the part/die interface. Furthermore, the lower die remained stationary, while a vertical displacement, determined experimentally, was applied to the upper die. Both dies were maintained at a temperature of 200/or 270 °C with the ambient temperature set at 50 and 70 °C, recorded at the industrial NSF process. Moreover, the billets were divided into two separate mesh zones (fine/coarsen mesh) to improve the simulation results while reducing the computational time, the average mesh size utilized in the billet was 1 mm. To further optimize computational efficiency and enhance simulation results, a remeshing strategy were implemented.

To incorporate the initial temperature distribution inside the billet before the deformation stage, the simulation process was divided into three main stages. Firstly, the cooling of the billet while transferring was simulated reproducing the movement from the furnace to the testing table. This stage accounts for the heat exchange with the surrounding air along the entire boundary surface of the billet. Following this, in the second stage, the evolution of temperature is simulated during the pre-compression holding time, when the billet is positioned on the lower die. Finally, in the third stage, the upper tool undergoes a predefined kinematic motion, and deformation occurs. The temperature distribution map for all components at the final stage of deformation is shown in Fig. 4. It is apparent from the Fig. 4 that maximum temperature can be recorded at the centre of the specimen throughout the process.

Test results

The adiabatic heating coefficient plays a crucial role in determining the amount of heat generated within the material during plastic deformation. This generated heat, in combination with heat transfer to the dies, surrounding air, and other factors, significantly influences the temperature of the workpiece throughout the forming process. As a result, variations in workpiece temperature can impact the required forming load and the flow behaviour of the material during the deformation. Additionally, the material flow during the deformation process can induce different levels of plastic deformation, consequently affecting the magnitude of heat generation. Therefore, understanding and accurately characterizing the AHC is essential for predicting and controlling temperature variations, forming loads, and material flow dynamics in the high temperature forming process.

To achieve this objective, it is important to evaluate the plastic deformation and temperature distribution throughout the entire forming process, considering not only the final outcome but also the evolution of these parameters over multiple strokes. Therefore, a comprehensive study is conducted, and the results are presented illustrating the 'temperature-plastic deformation' state of each point within the material at different stages of the process. By comparing scenarios under varying AHC such as 85AHC and 100AHC, insights into the influence of AHC on temperature and deformation profiles can be gained. This comparative analysis enables a deeper understanding of how changes in AHC affect the material behaviour and the temperature evolution during forming operations.

Adiabatic heating coefficient (AHC) specific analysis

After conducting all the simulations at the desired boundary conditions as stated in Table 1, the relation between the plastic strain and the deformation temperature is recorded. Given the study's focus to investigate the influence of the

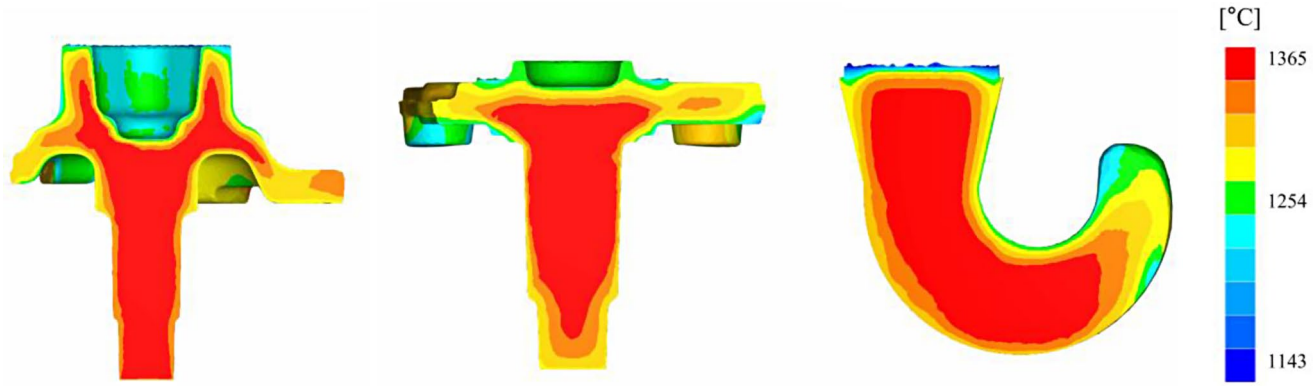

Fig. 4 Simulated temperature distribution map of 42CrMo at deformation temperature of 1360 °C (all benchmarks)

AHC throughout the process, various time steps were considered from the commencement to the end of each deformation stroke. As example, in the case of the H-spindle, the punch descended a stroke of 96.67 mm. This process was segmented into 10 strokes, evenly spaced from the start to the end of the process, denoted as 'stroke10' to 'stroke100'.

Low-bounds scenario

Figure 5 illustrates the relationship between temperature and equivalent plastic strain at different strokes, aiming to evaluate the proportion of plastic work converted into heat.

H-spindle

The overall results for the H-spindle are depicted in Fig. 5a, with the left figure showing the 3D view and the right one displaying the collapsed form. The initial observation reveals an expected trend: as the stroke of the process increases, the material undergoes progressively more deformation, resulting in a corresponding increase in equivalent plastic strain. The attained plastic strain value reaches up to 8, with some peak values slightly exceeding this threshold. Notably, considering that the billet was heated to 1360 ºC prior to transfer to the press, deformation occurs across a range of temperatures, spanning from 1100 ºC to 1350 ºC, with the majority of material deformation occurring between approximately 1200 ºC and 1320 ºC. Analysis of the data across the strokes reveals a consistent pattern: as the stroke increases, the temperature also tends to rise. This observed temperature increase could be attributed to the transfer of plastic work to adiabatic heating. This phenomenon becomes evident when examining the evolution of the minimum temperature values, which rise from 1100 ºC at a stroke of 20 to at least 1200 ºC at strokes of 100. Additionally, for this component, and likely related with the forming of the part, the evolution of plastic strain demonstrates an almost proportional relationship to the stroke.

When analysing the impact of the AHC, it's essential to compare the data obtained using 85AHC (represented by green dots) with that of 100AHC (depicted by red dots), considering that data points in where both simulations (85AHC and 100AHC) overlap are shown in light grey. A primary observation is that the majority of the deformed material exhibits a consistent pattern between both AHC values, as indicated by the overlapping areas in Fig. 5a-right. Notably, assuming a higher coefficient (100AHC) results in slightly higher temperatures in certain areas, particularly evident in strokes beyond 40, with an impact of approximately 10 ºC at most. However, the increase in temperature does not correspond to a significant increase in material flow, as the equivalent strain remains nearly unchanged for both AHCs values. While a larger deformation can be observed under 100AHC (indicated by red dots reaching up to 8 of plastic strain at 1325 ºC), larger outlier green points (85AHC) are also observed exceeding value of 9. Therefore, for the case of the H-spindle, assuming a low-bounds scenario, no significant impact is observed between assuming 85AHC and 100AHC.

R-spindle

The results for the R-spindle are illustrated in Fig. 5b. The maximum plastic strain value is recorded 15, at the last stroke of the deformation. Moreover, the minimum temperature value rise from 1030 ºC at the beginning of the process to 1100 ºC at the final stage. However, while evaluating the impact of the AHC, there is no noticeable difference across both AHC values, as can be seen from the overlapping areas in Fig. 5b-right. Although, at 85AHC slightly higher temperatures in certain areas are recorded while 100AHC is higher in some other areas, however this temperature increase does not result in a significant change in material flow, as the equivalent strain remains almost constant for both AHC values. Although for few points the greater deformation is observed, such as at 100AHC presented with red dots reaching up to the plastic strain value of 15 and for the 85AHC outlier in green reaching to 14. However, similar to H-spindle there is no major effect recorded due to change in AHC factor.

Hook

Lastly for Hook the same behaviour is noted, at the initial phase of the deformation, plastic strain values are observed to be low, gradually increasing as the deformation progresses. In Fig. 5c, it is evident that different AHC factors exhibit minimal effects. In short, the peak plastic strain value is recorded around 10. Although, a large difference is recorded between the minim temperature at initial and final strokes, however despite varying AHC factors, the minimum and maximum values of temperature and plastic strain remain almost identical, Fig. 5c right side. Overall, the results presented in Fig. 5 suggest that there is a minor effect of adiabatic heating on plastic strain and deformation temperatures during NSF testing conditions.

High-bounds scenario

H-spindle. Similarly, in the High-bounds scenario, Fig. 6 illustrates the relationship between plastic strain and temperatures. Unlike the Low-bounds scenario, these tests showcase a broader range of temperature data, spanning from approximately 400 °C to a peak value of around

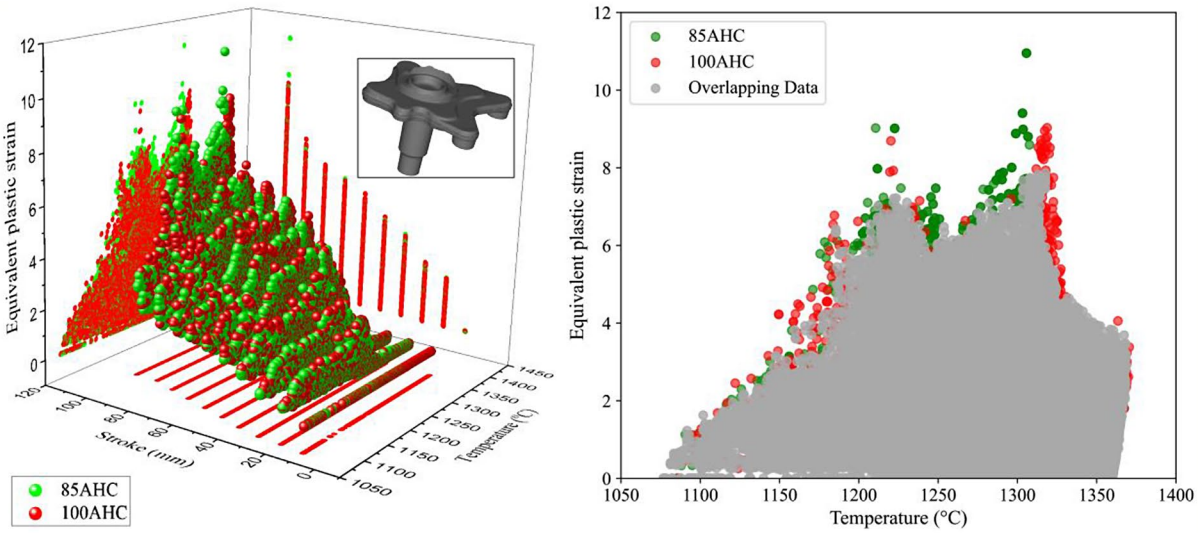

(a) H-spindle

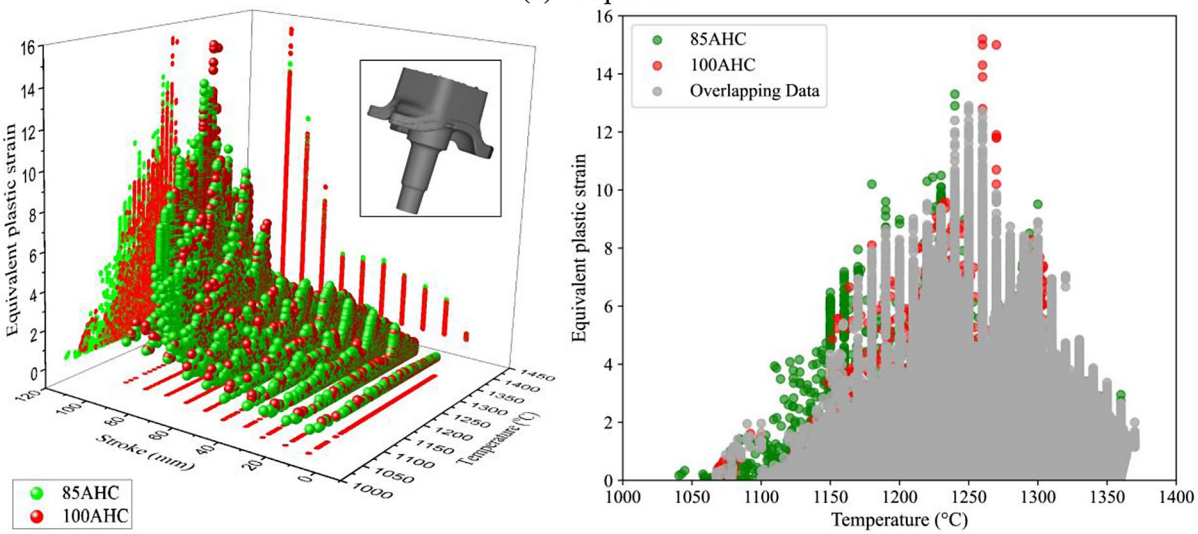

(b) R-spindle

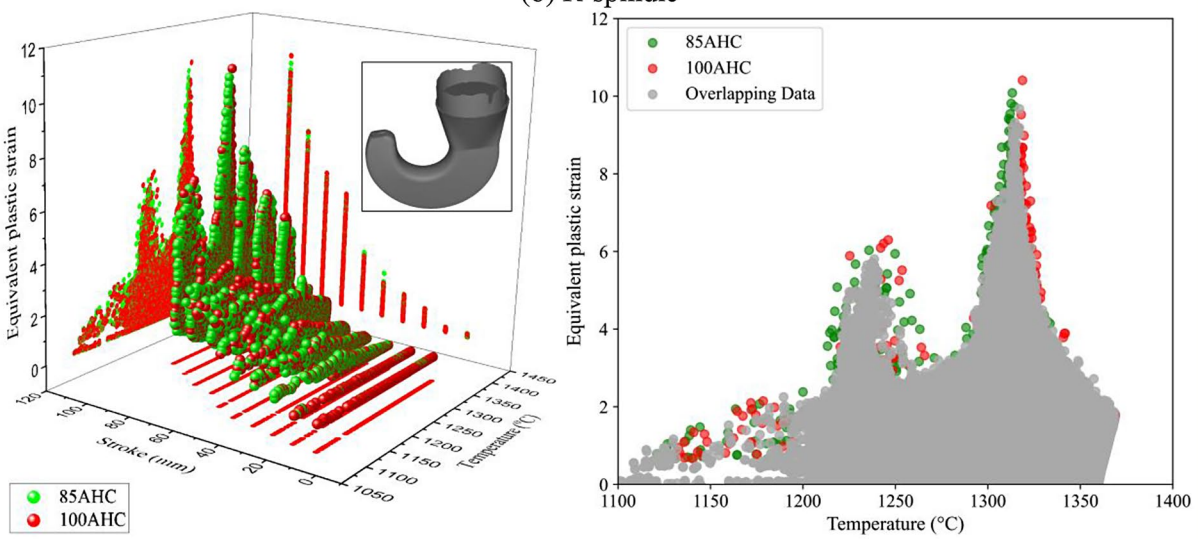

(c) Hook

Fig. 5 Plastic strain and temperature plots at 85AHC and 100 AHC value in all benchmarks (Low-bounds)

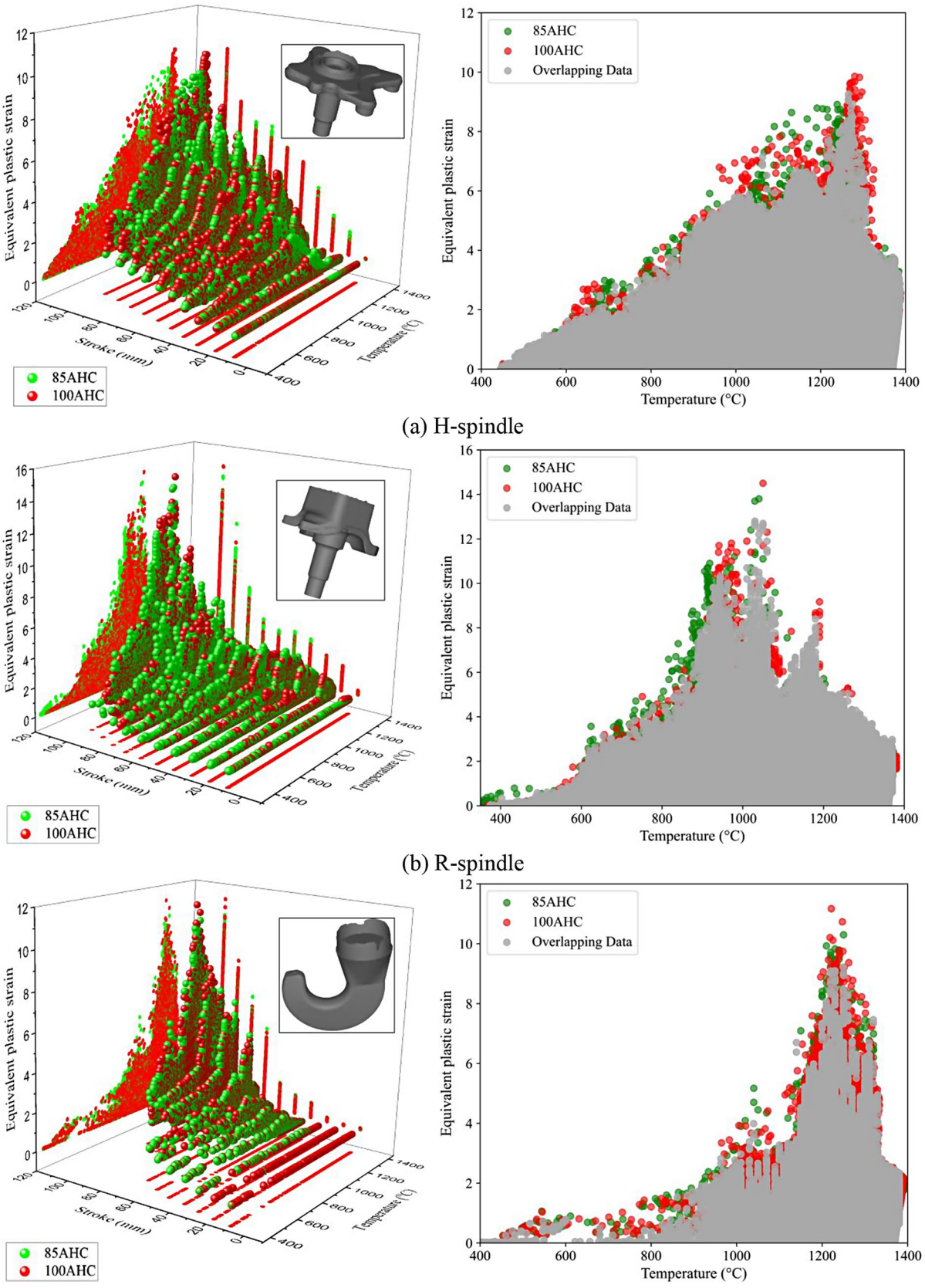

Fig. 6 Plastic strain and temperature plots at 85AHC and 100 AHC value in all benchmarks (High-bounds)

1390 °C. Additionally, plastic strain values are recorded at higher levels due to the different boundary conditions of the tests. For the H-spindle, the minimum temperature of the elements was recorded around 420 °C at stroke 10, increasing to 530 °C at the end of the deformation process (stroke 100). Conversely, elements with maximum temperatures either maintain or lose some heat throughout the process. Overall, at 100AHC the maximum equivalent plastic strain value was recorded approximately 10, whereas in the case of 85AHC, this value was slightly lower, as depicted in Fig. 6a, on the right side. Despite the minor effect of the AHC on the plastic strain, minimal to no effect was noted on the temperature profile in both testing conditions. This suggests that the AHC has little to no effect on the material behaviour during the forming process.

R-spindle. For the R-spindle in Fig. 6b, both AHC conditions exhibit a similar effect on the process, with the maximum value of plastic strain recorded around 15. While a few elements exceed this threshold, the majority behave similarly. Interestingly, unlike previous cases, the minimum temperature in the process increased from 350 °C to 450 °C at the end of the deformation stroke, indicating significant adiabatic heat generation. However, elements with the maximum temperature remained consistent. Additionally, the global temperature rise due to variation in the AHC value is minimal, with the maximum difference recorded around 10 °C. Importantly, the impact of AHC on material behaviour is negligible, as there is no significant difference in plastic strain value and temperature recorded during the test.

Hook. Finally, the results of the Hook benchmark are presented in Fig. 6(c), revealing a peak plastic strain value of 11.8 recorded during the final strokes of deformation. Additionally, adiabatic heating significantly increases the minimum temperature in the Hook benchmark compared to the other two benchmarks. The temperature rises from 400 °C at the initial strokes to 750 °C at the end of the process. However, despite this considerable variation in the minimum temperature, the average temperature remains consistent throughout the process. Most importantly, the variation in temperature values due to the AHC factor is negligible, as depicted in the figure on the right side.

Overall, in all benchmarks case despite the higher values of peak temperatures and peak plastic strain, the effect of the adiabatic heating coefficient is found to be negligible in both cases. This observation suggests that the amount of heat generated (adiabatic heating) during the NSF process is minimal, and consequently, the amount of plastic work converted into heat is also negligible.

Adiabatic heating coefficient (AHC) global analysis

As explained before, the AHC test is conducted in three phases, and during the transfer phase the billet can lose some amount of heat due to the heat transfer with the air and also to the dies during deformation. Hence adiabatic heating during the process can be affected, therefore a global analysis is conducted to investigate the effect of adiabatic heating in areas of the billet where minor temperature loss is recorded during the initial phases of the process. Figure 7 represents the plastic strain and delta temperature plots at the centre of the billet. In the analysis the centre of the billet has been selected due to the fact that the other part of the billet loses it temperature quite fast once it comes in contact with the surrounding air and forming dies, while the temperature remained the same at the centre of the billet. Figure 7(a) presents the plastic strain data for all benchmarks at Low-bounds, where the peak plastic strain value is recorded 0.45, 1.35 and 2.1 for HS (H-spindle), RS (R-spindle) and HO (Hook) respectively. However, it is evident from plot that there is very minimal difference observed when the AHC factor is changed from 85AHC to 100AHC. Furthermore, a slight rise in the plastic strain value is noted at High-bounds Fig. 7(b), although the effect of AHC remained the same. Despite variations in the AHC factor, the differences in plastic strain are negligible, emphasizing the limited impact of AHC even at the centre of the deformed benchmarks.

Moreover, regarding change in temperatures due to adiabatic heating, at Low-bounds the maximum rise in temperature due to adiabatic heating is noted to be 6.3 °C for H-spindle, 4 °C for R-spindle and 8 °C for Hook, respectively. Similarly, in High-bounds these values were nearly double when compared to the Low-bounds. However, the difference in temperature at the centre of the billet due to the variation in AHC factor is again minimal. Although the maximum rise in temperature is noted for HS, where the temperature difference of 2.5 °C is found. Based on this data, it is concluded that the adiabatic heating coefficient has a very small effect on the material behaviour during NSF process. One major contributing factor to this observation could be the rapid cooling of the billet under NSF testing conditions. Hence as a result no excessive heat is generated and thus a minor portion of the plastic energy is converted heat.

The analysis presented in Figs. 5, 6 and 7 provides insights into the relationship between temperature, equivalent plastic strain, and the adiabatic heating coefficient in the context of the NSF testing conditions. For the H-spindle, R-spindle, and Hook benchmark, observations reveal a consistent trend: as the stroke of the process increases, there is a corresponding increase in material deformation and equivalent plastic strain. This is accompanied by a rise

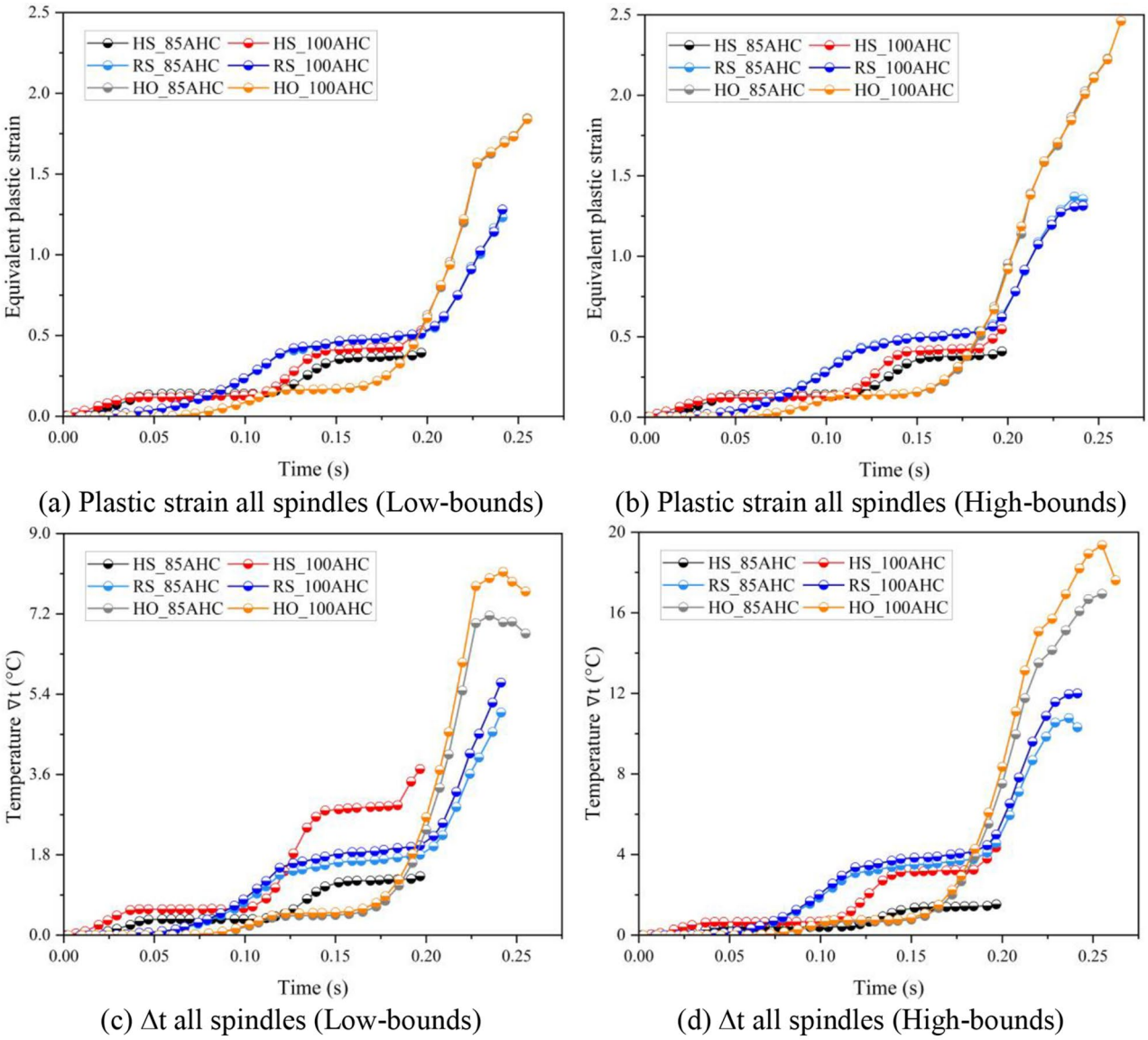

Fig. 7 Temperature change Δt and EQ strain recorded at the center of the billet (all benchmarks)

in temperature, attributed to the transfer of plastic work to adiabatic heating. While a higher AHC leads to slightly higher temperatures in some areas, the impact on material flow remains minimal. The behaviour is consistent across different AHC values and testing conditions, with negligible differences observed in plastic strain and temperature profiles. Even in the High-bounds scenario, where temperature and plastic strain values are higher, the effect of AHC remains insignificant. This suggests that the amount of heat generated during the NSF process, and consequently the conversion of plastic work into heat, is minimal. Overall, these findings highlight the negligible impact of AHC on material behaviour during NSF process, providing valuable insights for process optimization and control.

Conclusion

Prior to conducting experiments on the AHC, it is crucial to understand its effect during the NSF process. To achieve this goal, a sensitivity analysis of the AHC is conducted using FORGE NxT®. This analysis aims to numerically characterise the impact of adiabatic heating on the deformation behaviour of the material, focusing on plastic work. Three industrial benchmarks, namely the H-spindle, R-spindle, and Hook geometry are selected for this analysis. Each benchmark represents a unique geometry and material behaviour under NSF conditions. The sensitivity analysis is performed at two different levels of AHC to capture its varying effects on the deformation behaviour of each industrial component. The outputs of the sensitivity analysis are

successfully studied, and the results are presented in terms of temperature and equivalent plastic strain plots. These plots provide insights into the temperature distribution and plastic strain evolution throughout the NSF process under different AHC conditions. Under the scope of the studied three benchmarks, the main conclusions drawn from this study include:

1. The Adiabatic Heating Coefficient has a minimal effect on the deformation behaviour of 42CrMo4 steel at NSF condition for the studied benchmarks.
2. Despite variations in the AHC, the temperature and plastic strain profiles exhibit minor differences, indicating the robustness of the NSF process against adiabatic effects.
3. The rapid cooling of the billet under NSF testing conditions mitigates excessive heat generation, resulting in only a minor portion of the plastic energy being converted into heat.
4. Lastly the rise in temperature values is almost doubled in the case of High-bounds compared to Low-bounds, which is to be expected.

In summary, for the studied benchmarks, results suggest that the AHC has a minor effect on the process. Therefore, it does not seem necessary to invest resources in AHC characterization. It has to be considered that the present study is limited to the studied benchmarks and further studies are necessaries to extend this work to future geometries.

Author agreement

We declare that this manuscript entitled "The Influence of the Adiabatic Heating Coefficient on the Near Solidus Forming Process" is original, has not been published before and is not currently being considered for publication elsewhere.

We confirm that the manuscript has been read and approved by all named authors and that there are no other persons who satisfied the criteria for authorship but are not listed. We further confirm that the order of authors listed in the manuscript has been approved by all of us.

We understand that the Corresponding Author is the sole contact for the Editorial process. He is responsible for communicating with the other authors about progress, submissions of revisions and final approval of proofs.

Acknowledgements The authors would like to acknowledge the Exploration of high entropy alloys as substitute materials for sustainable mobility and decarbonisation (HEAPLAS) project funded by Ministerio de Ciencia e Innovación, with the reference PID2022-139130OA-I00, the HSSF, Hybrid Semi-Solid Forming project funded by the "Research Fund for Coal and Steel" (RFCS) program of the European union, with the grant number 800763, and the Procesos de Fabricación de Excelentes para propiedades máximas (PROMAX), funded by Basque Government through the ELKARTEK funding scheme (reference KK-2020/00087).

Author contributions Muhammad Sajjad: Methodology, Investigation, Software, Formal analysis, Validation, Visualization, Writing – original draft. Julen Agirre: Methodology, Investigation, Formal analysis. Gorka Plata: Conceptualization, Methodology, Investigation, Writing – review & editing. Jokin Lozares: Conceptualization, Methodology, Investigation, Writing – review & editing, Resources. Joseba Mendiguren: Conceptualization, Resources, Supervision, Project administration, Writing – review & editing.

Funding Open Access funding provided thanks to the CRUE-CSIC agreement with Springer Nature.

Data availability All data supporting the findings of this study are included within the paper and its Supplementary Information. Additional data if required, are available from the corresponding author upon request.

Declarations

Competing interest The authors declare that they have no known competing financial interests or personal relationships that could have appeared to influence the work reported in this paper.

Declaration of Generative AI and AI-assisted technologies in the writing process During the preparation of this work the author(s) used Chat GTP Open AI 3.5 for the re-write of the text to improve its quality. After using this tool, the author(s) reviewed and edited the content as needed and take(s) full responsibility for the content of the publication

References

1. Plata G, Lozares J, Sánchez A et al (2020) Preliminary study on the capability of the novel near solidus forming (NSF) technology to manufacture complex steel components. Materials 13:1–14. https://doi.org/10.3390/ma13204682
2. Klitschke S, Trondl A, Huberth F, Liewald M (2018) Adiabatic heating under various loading situations and strain rates for advanced high-strength steels. IOP Conf Ser Mater Sci Eng 418:012123. https://doi.org/10.1088/1757-899X/418/1/012123
3. Larour P (2010) Strain rate sensitivity of automotive sheet steels: influence of plastic strain, strain rate, temperature, microstructure, bake hardening and pre-strain. Aachen, Techn. Hochsch., Diss, Zugl.

4. Pantleon W, Francke D, Klimanek P (1996) Modelling adiabatic heating during high-speed deformation. Comput Mater Sci 7:75–81. https://doi.org/10.1016/S0927-0256(96)00063-8
5. Soares GC, Patnamsetty M, Peura P, Hokka M (2019) Effects of Adiabatic Heating and strain rate on the dynamic response of a CoCrFeMnNi High-Entropy Alloy. J Dynamic Behav Mater 5:320–330. https://doi.org/10.1007/s40870-019-00215-w
6. Langi V, Soares GC, Ahmed S et al (2023) Effects of strain rate and adiabatic heating on mechanical behavior of medium manganese Q&P steels. Mater Sci Engineering: A 865:144659. https://doi.org/10.1016/j.msea.2023.144659
7. Murillo-Marrodán A, Bulzak T, García E et al (2024) Effect of warm forming process parameters on 42CrMo4 skew rolled bar mechanical properties and microstructure. Archives Civil Mech Eng 24:90. https://doi.org/10.1007/s43452-024-00902-z
8. Sela A, Ortiz-de-Zarate G, Soler D et al (2023) Adiabatic self-heating determination for Ti6Al4V at different temperatures. Int J Heat Mass Transf 204:123747. https://doi.org/10.1016/j.ijheatmasstransfer.2022.123747
9. Krawczyk J, Łukaszek-Sołek A, Śleboda T et al (2023) Tool wear issues in Hot forging of Steel. Materials 16:471. https://doi.org/10.3390/ma16020471
10. Lozares J, Plata G, Hurtado I et al (2020) Near solidus forming (NSF): semi-solid steel forming at high solid content to obtain as-forged properties. Met (Basel) 10. https://doi.org/10.3390/met10020198
11. Jin Y, Xi C, Xue P et al (2020) Constitutive model and microstructure evolution finite element Simulation of multidirectional forging for GH4169 superalloy. Met (Basel) 10:1695. https://doi.org/10.3390/met10121695
12. Khawarizmi RM, Lu J, Nguyen DS et al (2022) The Effect of Ti-6Al-4V microstructure, cutting speed, and adiabatic heating on segmented chip formation and Tool Life. JOM 74:526–534. https://doi.org/10.1007/s11837-021-05091-1
13. Yeom J-T, Kim JH, Hong J-K et al (2012) Prediction of microstructure evolution in Hot Backward Extrusion of Ti-6Al-4V Alloy. J Metall 2012:1–6. https://doi.org/10.1155/2012/989834
14. Hodowany J, Ravichandran G, Rosakis AJ, Rosakis P (2000) Partition of plastic work into heat and stored energy in metals. Exp Mech 40:113–123. https://doi.org/10.1007/BF02325036
15. Mason JJ, Rosakis AJ, Ravichandran G (1994) On the strain and strain rate dependence of the fraction of plastic work converted to heat: an experimental study using high speed infrared detectors and the Kolsky bar. Mech Mater 17:135–145. https://doi.org/10.1016/0167-6636(94)90054-X
16. Kapoor R, Nemat-Nasser S (1998) Determination of temperature rise during high strain rate deformation. Mech Mater 27:1–12. https://doi.org/10.1016/S0167-6636(97)00036-7
17. Hodowany J (1998) On the partition of plastic work into heat and stored energy in metals; part I. Experiments
18. Gao N (2008) Applications of Differential scanning calorimetry on materials subjected by severe plastic deformation. Mater Sci Forum 584–586:255–260. https://doi.org/10.4028/www.scientific.net/MSF.584-586.255
19. Owolabi G, Odoh D, Peterson A et al (2013) Measurement of the Deformation of Aluminum Alloys under high strain Rates using high speed Digital Cameras. World J Mech 03:112–121. https://doi.org/10.4236/wjm.2013.32009
20. Knysh P, Korkolis YP (2015) Determination of the fraction of plastic work converted into heat in metals. Mech Mater 86:71–80. https://doi.org/10.1016/j.mechmat.2015.03.006
21. Härtel S, Graf M, Awiszus B et al (2018) Novel Approach for the determination of the Taylor-Quinney Coefficient. Mater Sci Forum 918:103–109. https://doi.org/10.4028/www.scientific.net/MSF.918.103
22. Chadha K, Shahriari D, Jahazi M (2018) An Approach to develop hansel–spittel constitutive equation during Ingot Breakdown Operation of Low Alloy Steels. Frontiers in materials Processing, Applications, Research and Technology. Springer Singapore, Singapore, pp 239–246
23. Sajjad M, Trinidad J, Plata G et al (2024) Sensitivity analysis of near solidus forming (NSF) process with digital twin using Taguchi approach. Adv Manuf. https://doi.org/10.1007/s40436-024-00482-4
24. Muhammad Sajjad G, Plata J, Lozares J (2023) Mendiguren Digital twin development for the sensitivity analysis of near solidus forming process. In: Materials Research Forum LLC. pp 1521–1530
25. Sajjad M, Agirre J, Plata G et al (2024) Characterization of the heat transfer coefficient at near solidus forming condition using columnar pressing test. Int J Adv Manuf Technol 135:721–733. https://doi.org/10.1007/s00170-024-14531-6